Electronic Supplementary Material (ESI) for Journal of Materials Chemistry B.

Supporting Information

Layer-by-Layer Assembly of Polyoxometalate-Pyrene-Decorated Fluorescent Microspheres for Suspension Immunoassay of *Listeria Monocytogenes*

Wen Ju[a†], Xiuling Song[a†], Gang Yan[b†], Kun Xu[a], Juan Wang[a], Dehui Yin[a], Li Li[a], Xiaofeng Qu[a], Yangguang Li[b*], Juan Li[a*]

[a.] *College of Public Health, University of Jilin, Changchun, 130021, China;* [b.] *Key laboratory of Polyoxometalate Science of Ministry of Education, Faculty of Chemistry, Northeast Normal University, Changchun, 130024, China*

1 Crystal structural data and figures

2 Additional physical measurements

3 Additional *LM* detection experiments

1. Crystal structural figures and data of POM-pyrene 1

The single-crystal X-ray diffraction analysis shows that compound 1 crystallizes in the monoclinic C2/c space group. The structural unit of compound 1 consists of one $[V_6O_{13}\{(OCH_2)_3CNH\text{-}CH_2\text{-}C_{16}H_9\}_2]_2$- hybrid polyoxoanion and two TBA+ counter cations. In the hybrid polyoxoanion of 1, the central inorganic cluster $\{V_6O_{19}\}$ shows a typical Lindqvist-type structure, in which six $\{VO_6\}$ octahedra are connected with each other in an edge-sharing mode. Theoretically, $\{V_6O_{19}\}$ moiety possesses eight negative charges, however, the introduction of two Tris ligands on the surface of $\{V_6O_{19}\}$ fragment brings six sharing O atoms between POM and Tris units (see Fig. S1 and Fig. S2), dramatically decreases the negative charges of the hybrid molecule, and stabilize the whole $\{V_6O_{19}\}$ unit. Based on the covalent connections between POM and Tris linkers, two pyrene groups are introduced into the inorganic POM units, forming a butterfly-type hybrid molecule with two negative charges. It is noteworthy that the introduction of Tris(hydroxymethyl) groups into POM unit led to two types of V-O bond lengths. The bond lengths of V-Ocarbon range from 2.002(4) to 2.026(4)Å, while the bond lengths of V-O POM are in the range of 1.810(4)-1.825(4)Å. In the packing arrangement, the adjacent hybrid molecules are stacked together by the obvious π-π interactions between two adjacent parallel pyrene planes derived from different POM-pyrene hybrid molecules as wellas extensive weak C-H…O intermolecular interactions between POM units and adjacent pyrene groups, forming the 3-D supramolecular open framework with 1-D channels along c axis (Fig. S3 and Fig. S4). The short vertical distance between two adjacent pyrene planes is ca. 3.259Å (Fig. S5). The channels are filled with TBA+ cations, charge-balancing the whole negative supramolecular framework.

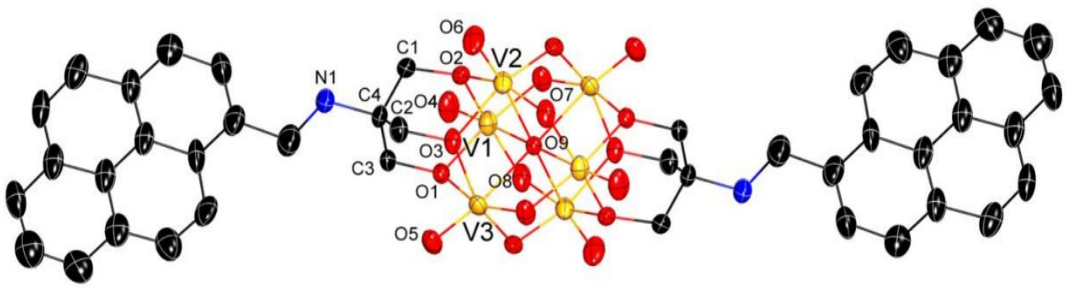

Fig. S1 ORTEP diagram of the structure of POM-pyrene **1** with thermal ellipsoids at 30% probability

displacement. All H atoms are omitted for clarity.

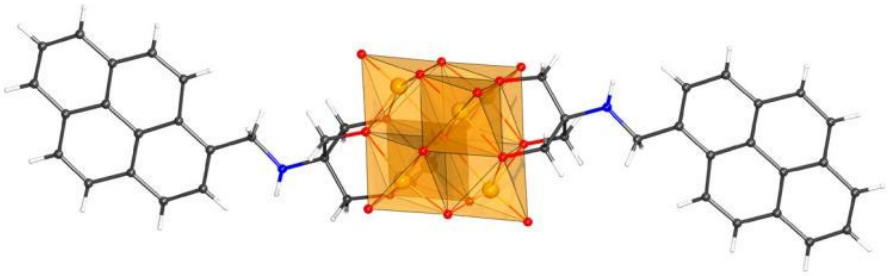

Fig. S2 Polyhedral and ball-and-stick view of the structure of POM-pyrene 1

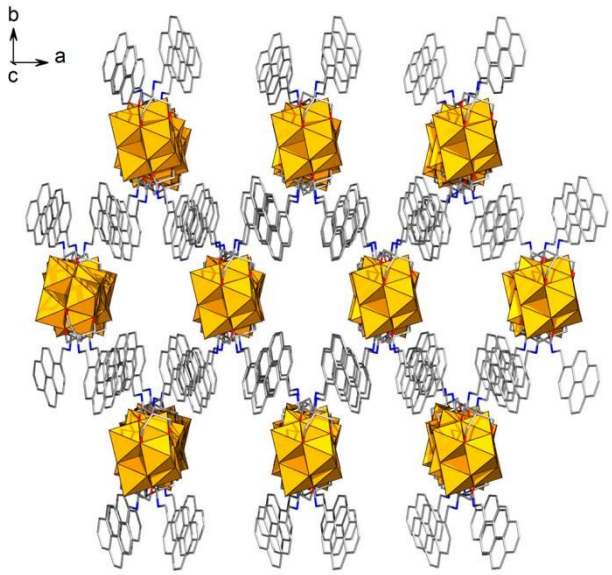

Fig. S3 Packing arrangement of POM-pyrene in compound 1 viewed along c axis. H atoms and TBA+ cations are omitted for clarity.

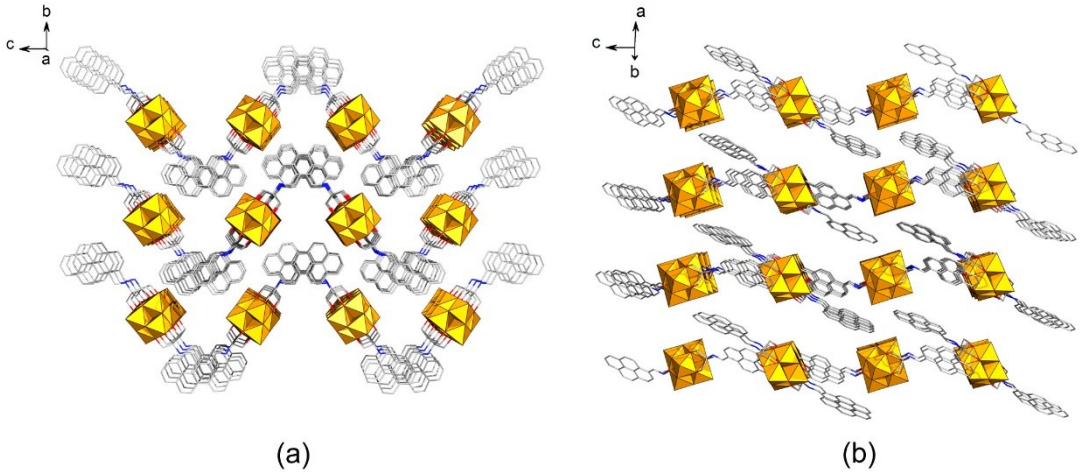

Fig. S4 Packing arrangement of POM-pyrene units in the crystal structure of 1 viewed along **(a)** *a* axis and **(b)** *b* axis. All H atoms and TBA^+ cations are omitted for clarity.

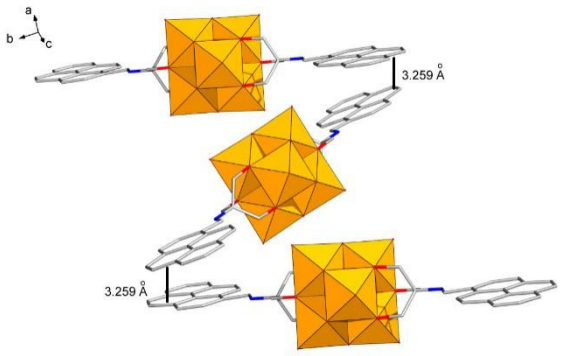

Fig. S5 Intermolecular π…π interactions between two pyrene groups from adjacent hybrid POM-pyrene units. The short distance between two pyrene planes is 3.259 Å.

Diffractive quality single crystal of compound 1 was mounted on a glass fiber and the crystallographic data of 1 was collected at 150(2) K on a Rigaku R-axis Rapid IP diffractometer using graphite monochromatic Mo-Kα radiation (λ = 0.71073 Å) and the IP technique. A multi-scan adsorption correction method was used. The structure of 1 was solved by the direct method and refined by the full-matrix least-squares method on F2 using the SHELXTL-97 crystallographic software package. Anisotropic thermal parameterswere used to refine non-hydrogen atoms. Hydrogen atoms on the organic C centers were included in the refinement riding on their respective parent C atoms. The crystal data and structure. refinement result of POM-pyrene 1 is summarized in Table S1.

Table S1 Crystal data and structure refinements for compound **1**.

Empirical formula	$C_{74}H_{108}N_4O_{19}V_6$
Formula weight	1663.28
T (K)	150(2)
λ (Å)	0.71073
Crystal system	monoclinic
Space group	*C2*/c
a (Å)	12.5396(2)
b (Å)	24.454(2)
c (Å)	25.013(2)
β (°)	93.069(2)
V (Å^3)	7658.9
Z	4
D_{calcd} (g cm^{-3})	1.442
Absorption coefficient (mm^{-1})	0.774
F (000)	3480
ϑ range (°)	1.67-25.00
Reflections collected	19461
Unique reflections/(R_{int})	6742/0.0617
GOF	1.001
R_1 (I>2σ)[a]	0.0682
wR_2 (all data)[b]	0.1654

Note: [a]$R_1 = \Sigma||F_o| - |F_c||/\Sigma|F_o|$; [b]$wR_2 = \Sigma[w(F_o^2 - F_c^2)^2]/\Sigma[w(F_o^2)^2]^{1/2}$.

Table S2 Selected bond lengths (A) and angles () of POM-pyrene **1**

V(1)-O(4)	1.594(4)	V(2)-O(6)	1.585(4)
V(1)-O(8)	1.810(4)	V(2)-O(10)	1.816(4)
V(1)-O(7)	1.825(4)	V(2)-O(8)	1.823(4)
V(1)-O(1)#1	2.002(4)	V(2)-O(2)	2.009(4)
V(1)-O(2)#1	2.011(4)	V(2)-O(3)	2.026(4)
V(1)-O(9)	2.2280(10)	V(2)-O(9)	2.2374(10)
V(3)-O(5)	1.589(4)	V(3)-O(1)	2.004(4)
V(3)-O(10)#1	1.812(4)	V(3)-O(3)	2.021(4)
V(3)-O(7)	1.815(4)	V(3)-O(9)	2.2302(10)
O(4)-V(1)-O(9)	172.68(18)	O(6)-V(2)-O(9)	172.40(18)
O(8)-V(1)-O(9)	81.50(14)	O(10)-V(2)-O(9)	81.33(13)
O(7)-V(1)-O(9)	81.20(13)	O(8)-V(2)-O(9)	80.96(13)
O(1)#1-V(1)-O(9)	77.49(11)	O(2)-V(2)-O(9)	77.24(12)
O(2)#1-V(1)-O(9)	77.41(12)	O(3)-V(2)-O(9)	77.41(11)
O(5)-V(3)-O(9)	171.91(17)	O(1)-V(3)-O(9)	77.39(11)
O(10)#1-V(3)-O(9)	81.62(13)	O(3)-V(3)-O(9)	77.67(12)
O(7)-V(3)-O(9)	81.34(13)		

Symmetry transformations used to generate equivalent atoms: #1 -x+2,-y+1,-z+1

2. Additional physical measurements

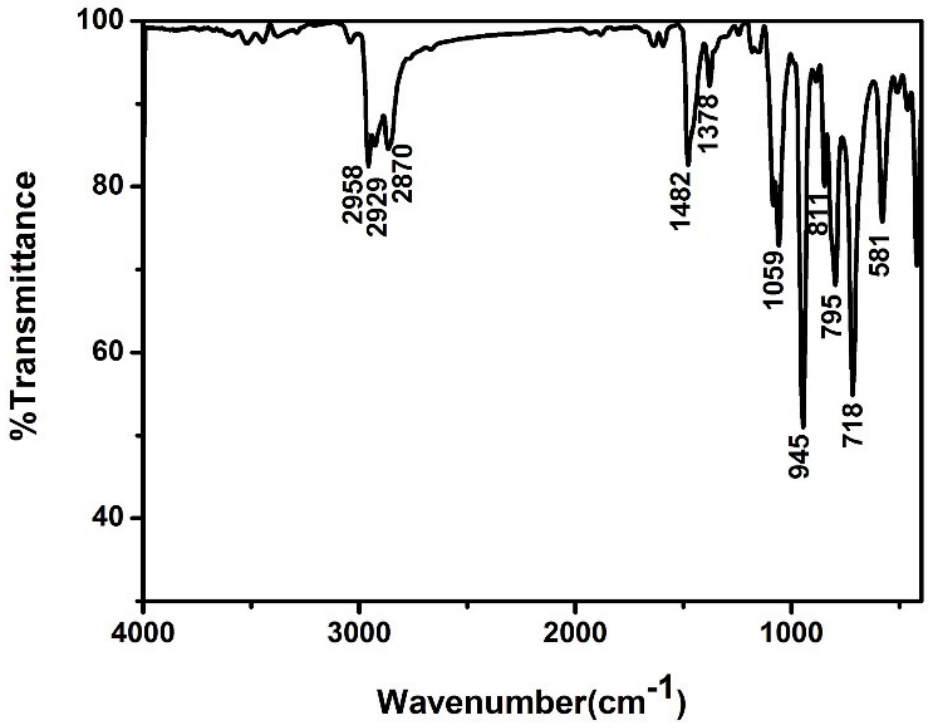

Fig. S6 IR spectrum of compound **1**

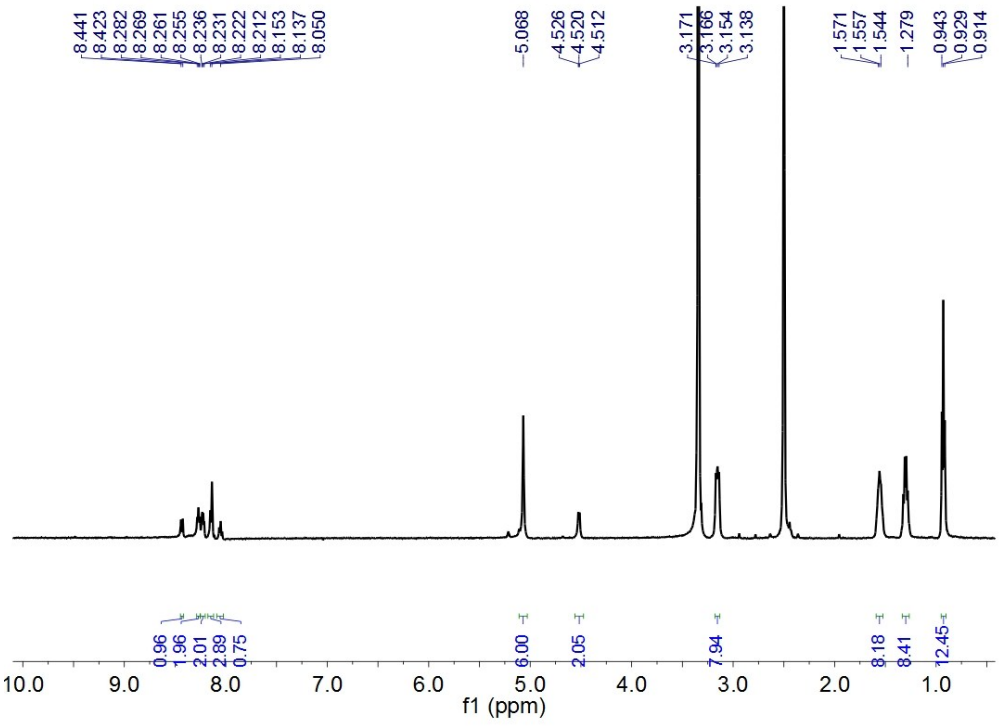

Fig. S7 ^{1}H NMR of compound **1** in DMSO. ^{1}H NMR (500 MHz,) δ 8.43 (d, *J* = 9.0 Hz, 1H), 8.27 (t, *J* = 7.0 Hz, 2H), 8.24 – 8.22 (m, 2H), 8.14 (d, *J* = 8.0 Hz, 3H), 8.05 (t, *J* = 7.5 Hz, 1H), 5.07 (s, 6H), 4.52 (d, *J* = 7.0 Hz, 2H), 3.17 – 3.14 (m, 8H), 1.57 – 1.54 (m, 8H), 1.34 – 1.27 (m, 8H), 0.93 (t, *J* = 7.5 Hz, 12H).

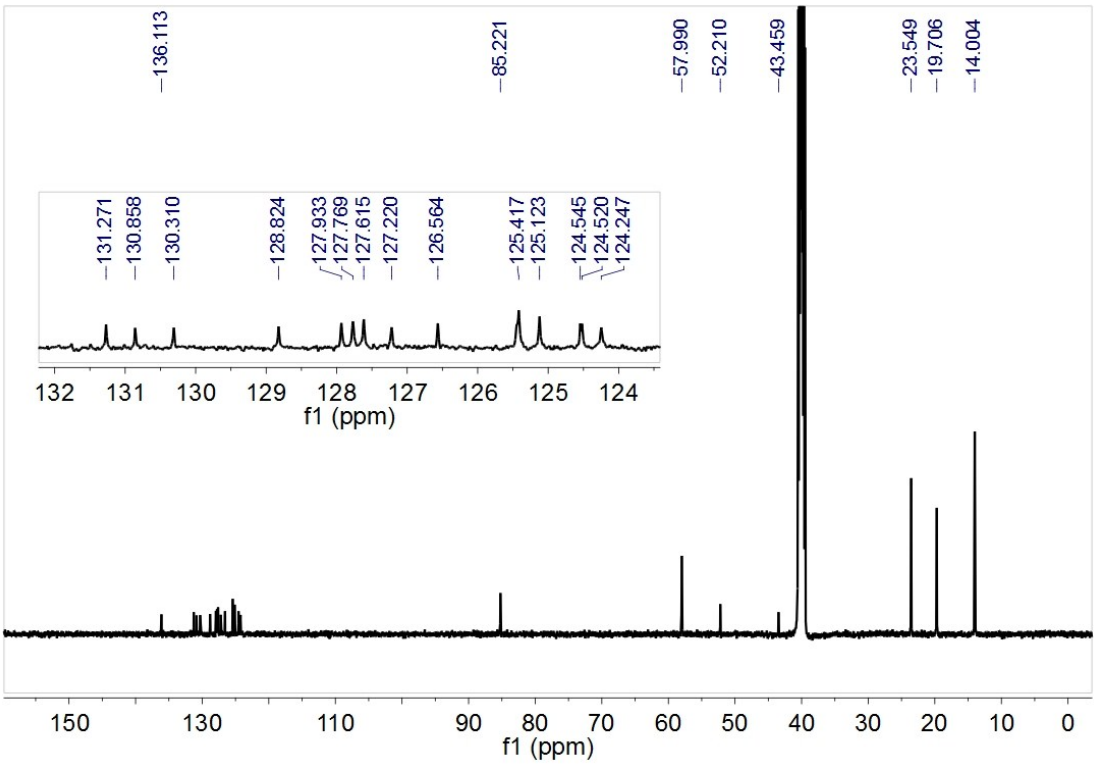

Fig. S8 ^{13}C NMR of compound **1** in DMSO. ^{13}C NMR (125 MHz, DMSO) : δ 136.1, 131.23, 130.9, 130.3, 128.8, 127.9, 127.8, 127.6, 127.2, 126.6, 125.4, 125.1, 124.6, 124.5, 124.3, 85.2, 58.0, 52.2, 43.5, 23.6, 19.7, 14.0.

3 Additional LM detection experiments

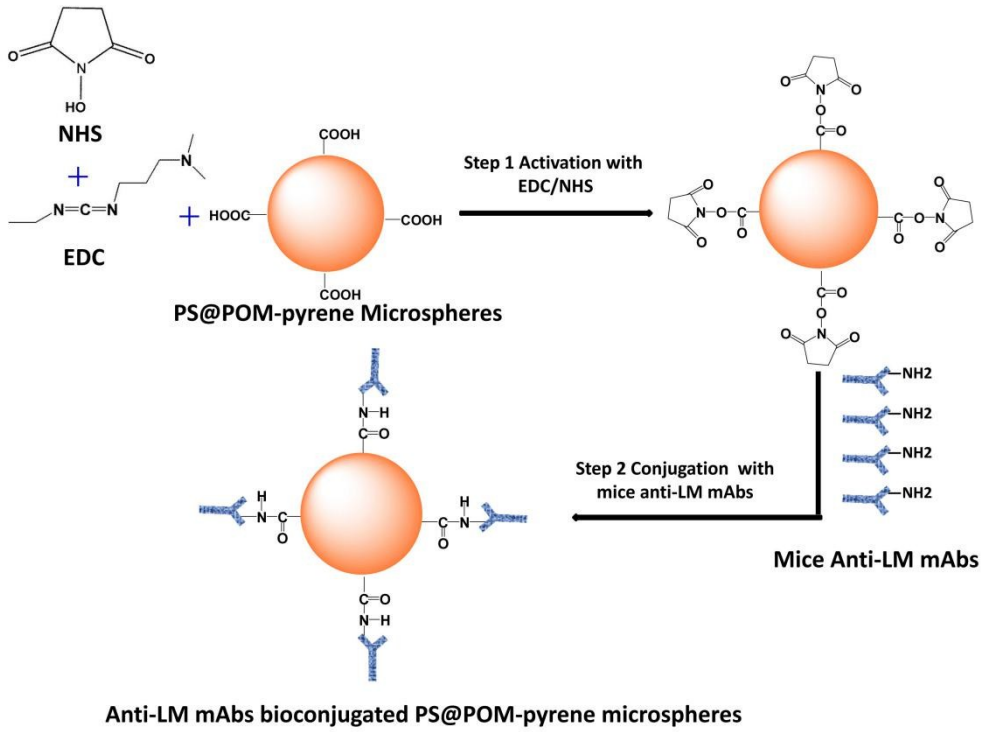

Scheme S1 Schematic view of biofunctionalization steps of PS@POM-pyrene microspheres conjugated with anti-*LM* mAbs

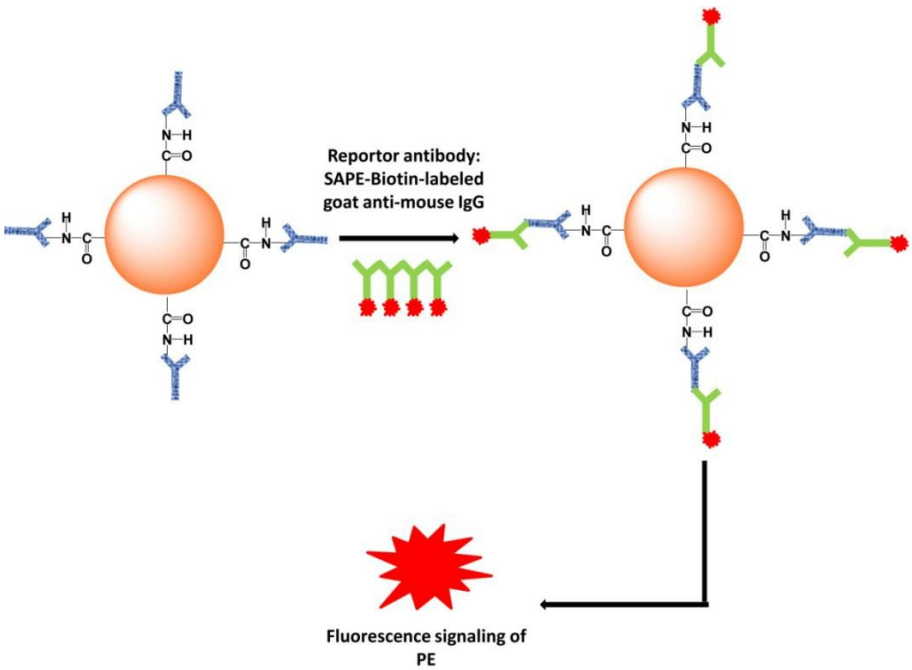

Scheme S2 Schematic view of working principle of fluorescence microsphere-based suspension immunoassay

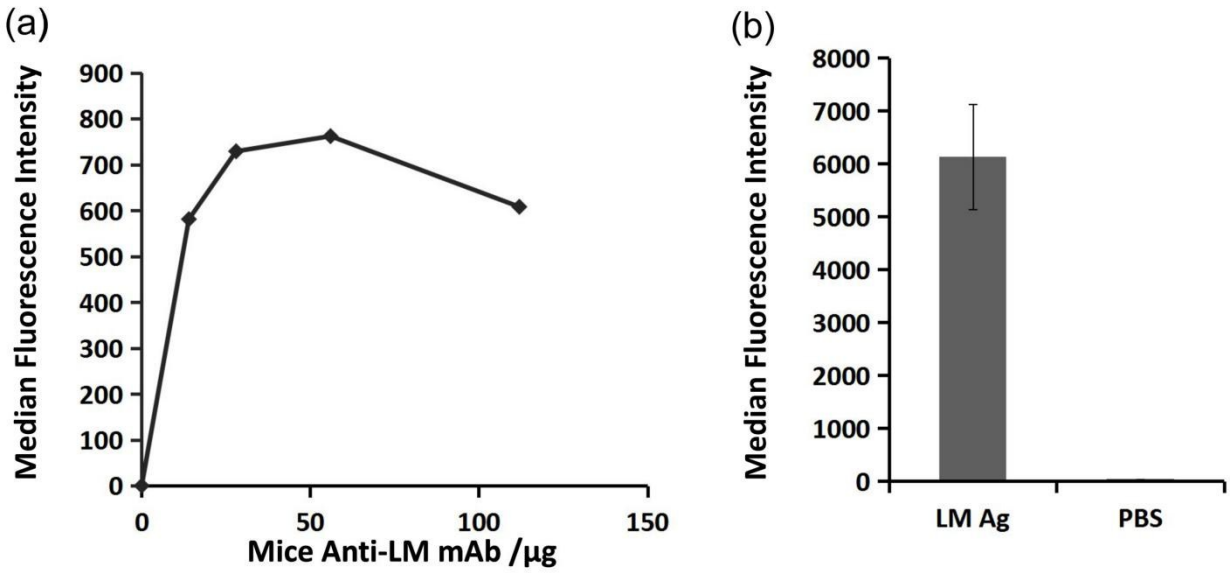

Fig. S9(a) The change of MFI values when different amounts of mice anti-*LM* mAb were used for coupling with 10^6 PS@POM-pyrene microspheres in the binding assay. The MFI values was increased when more mAb was coupled on the surface of the microspheres. **(b)** Median fluorescence intensity (MFI) values of the fluorescence microspheres incubated with *LM* Ag (n=5) and no *LM* Ag (PBS only, n=5) based on FCM measurements. During the measurement, the immunodiagnostic complex with fluorescently labeled streptavidin-PE is obtained. *LM* Ag samples incubated with anti-*LM* mAbs bioconjugated $\mathbf{P_6}$ microspheres showed high MFI values, while low MFI value of PBS samples was detected.

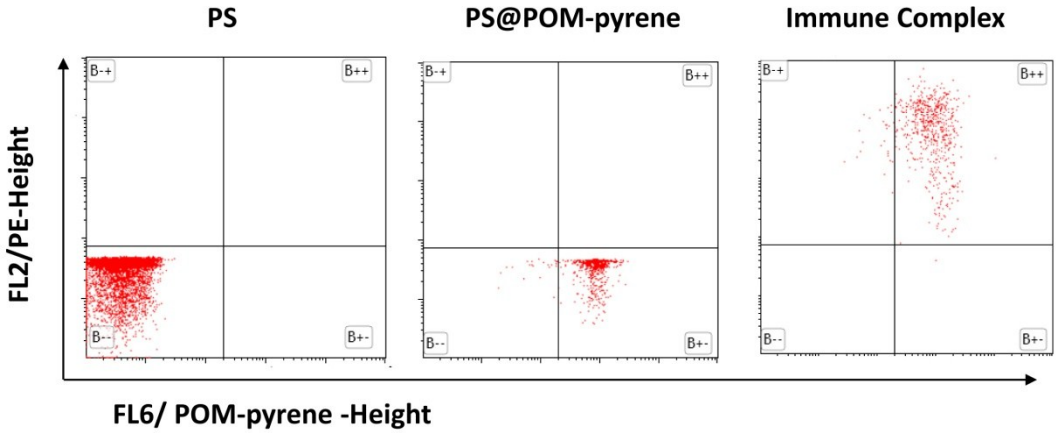

Fig. S10 Flow cytometry of PS (POM-pyrene negative and PE positive), PS@POM-pyrene (POM-pyrene positive and PE negative and Immune complex (POM-pyrene positive and PE negative)

Table S3. Repeatability of PS@POM-pyrene used for detecting *LM* Ag

	LM-sample 1	*LM*-sample 2	PBS
MFI-1	5560	3723	42
MFI-2	5314	3540	44
MFI-3	5560	3703	44
Mean	5478.00	3655.33	43.33
S	115.97	81.96	0.94
CV%	2.12	2.24	2.18